J Nanostruct 13(4): 902-914, Autumn 2023

RESEARCH PAPER

Nickel and Cadmium Sulfide/Chitosan Nanocomposites: Synthesis, Characterization and Applications

Azam Sobhani

Department of Chemistry, Kosar University of Bojnord, Bojnord, 94531–55168, Iran

ARTICLE INFO

Article History:
Received 20 July 2023
Accepted 22 September 2023
Published 01 October 2023

Keywords:
Adsorption
Cadmium sulfide
Chitosan
Nickel sulfide
Nanocomposite

ABSTRACT

Water pollution on account of textile industrial effluents represents a serious environmental problem which is increasing day by day. This study reports the synthesis of metal sulfide/chitosan nanocomposites (MS/chit NCs), M=Ni, Cd, via three steps: (1) synthesis of M(Tu) complex, Tu=thiourea, by a simple reflux route, employing metal nitrates and thiourea as the reactants (2) synthesis of MS nanostructures by simple thermal decomposition method using [M(Tu)] as precursors (3) synthesis of MS/chitosan nanocomposites. The fabricated nanostructures and nanocomposites were characterized by X-ray diffraction (XRD), Fourier-transform infrared spectroscopy (FT-IR), scanning electron microscopy (SEM) and energy-dispersive X-ray spectroscopy (EDS). The adsorption is one of the most efficient techniques for removing the pollution from the solvent phase. The nanocomposites synthesized in this work could help to solve the waste disposal problem. They were applied for the MB removal from aqueous solution. The intensity of peaks of MB were decreased after their adsorption on the surface of the nanocomposites in UV-Vis spectra.

How to cite this article
Sobhani A. Nickel and Cadmium Sulfide/Chitosan Nanocomposites: Synthesis, Characterization and Applications. J Nanostruct, 2023; 13(4):902-914. DOI: 10.22052/JNS.2023.04.001

INTRODUCTION

Transition metal sulfides exhibit interesting optical, electronic, thermoelectric and photoelectric properties [1–7]. Nickel sulfide an important member of this large family, finds use as a potential cathode material for the rechargeable lithium battery, as a catalyst in the degradation of organic dyes and in magnetic devices [8, 9]. It is an inorganic compound with the formula NiS_x. These compounds range in color from bronze (Ni_3S_2) to black (NiS_2). The nickel sulfide with simplest stoichiometry is NiS, also known as the mineral millerite. Nickel sulfide is a p-type semiconductor with a narrow band gap of about 0.5 eV and is most efficient electrochemically active materials due to its variety of applications such as lithium ion batteries, supercapacitors, photocatalytic H_2 generation and solar cells [10]. As a representative II–VI semiconductor, CdS with a direct band gap of 2.42 eV is considered to be an excellent material for various optoelectronics applications in the visible-light range, including nonlinear optical devices, LEDs and solar cells [11, 12].

During the last decade, many researchers have focused on heterogeneous catalysis techniques instead of homogeneous catalysts for the degradation of organic pollutants [13]. Water pollution on account of textile industrial effluents represents a serious environmental problem which is increasing day by day. Currently, the use of natural polymers (including proteins and polysaccharides) is broadly developed. Polysaccharides are a large

* *Corresponding Author Email: sobhani@kub.ac.ir*

group of biopolymers that have many properties like biodegradability, environmentally friendly, inexpensiveness, and availability. Alginate, cellulose, starch, gum, pectin, chitin, and chitosan are the most important types of polysaccharides [14]. In this work, we use chitosan for the synthesis of MS/chit NCs. The as-prepared nanocomposites help us to remove MB from the aqueous solution. After cellulose, chitosan is the next most sufficient polymer originating from a deacetylated variant of the naturally occurring amino polysaccharide chitin. Compared with other stabilized supports, the chitosan biopolymers and its composites have been widely used for the removal of toxic organic pollutants from wastewater. MB is a cationic dye, biologically dangerous and control of its content is necessary [15]. Elimination of dye pollution from the solvent phase by adsorption is a necessary aspect of research [16-20]. This research is the first study comparing the synthesis of nickel and cadmium sulfides via thermal decomposition under different conditions and comparing their application for removing MB from aqueous solutions.

MATERIALS AND METHODS

Materials and Characterization

$Ni(NO_3)_2.6H_2O$, $Cd(NO_3)_2.4H_2O$ and thiourea ($H_2N{-}C(=O){-}NH_2$) were provided from Merck company and used as received. A Philips XpertPro diffractometer with Ni-filtered Cu Kα radiation and λ = 1.54 Å was used to identify the phase

Table 1. The reaction conditions of MS nanostructures and MS/chitosan nanocomposites synthesized in this work.

Sample no.	Precursors	Surfactant	T and t of thermal decomposition
1	$Ni(NO_3)_2$ + Tu	–	500 ˚C , 4 h
2	$Ni(NO_3)_2$ + Tu	CTAB	500 ˚C , 4 h
3	$Ni(NO_3)_2$ + Tu	PVA	500 ˚C , 4 h
4	$Ni(NO_3)_2$ + Tu	PEG	500 ˚C , 4 h
5	$Cd(NO_3)_2$ + Tu	–	500 ˚C , 4 h
6	$Cd(NO_3)_2$ + Tu	CTAB	500 ˚C , 4 h
7	$Cd(NO_3)_2$ + Tu	PVA	500 ˚C , 4 h
8	$Cd(NO_3)_2$ + Tu	PEG	500 ˚C , 4 h
9	Sample 2 + chitosan	–	–
10	Sample 4 + chitosan	–	–
11	Sample 6 + chitosan	–	–

T = Temperature, t = time

and study XRD patterns. The morphology of the products was studied by field emission scanning electron microscope (TESCAN Mira3 FE-SEM). SEM microscope was also used to investigate the EDS spectrum. Fourier transform infrared spectrum (FTIR) was taken by a Nicolet IS 10 spectrophotometer made by the American Thermo scientific company. A Evolution 300 spectrophotometer made in the American Thermo scientific company was used to study UV-Vis spectra in photocatalytic studies.

Synthesis of [M(tu)] complex

[M(tu)] complex, as precursor, was synthesized according to this procedure: metal nitrate salt, 2 mmol, was dissolved in distilled water. Then surfactant, including CTAB, PVA and PEG, was added to the solution under stirring. The mixture was refluxed at 120˚C for about 1h. In the next step, a solution of thiourea, 2 mmol, was dissolved in distilled water and dropwise added into the above solution under magnetic stirring. After addition of all the reagents, the mixture was refluxed at 120 °C for 1h. With evaporation of the solution, a solid was recovered, filtered, washed with distilled water and ethanol and dried.

Synthesis of MS nanostructures

Nickel and cadmium sulfide nanostructures were prepared by the thermal decomposition method from [M(Tu)], in a furnace at 500 ˚C for 4h.

Synthesis of MS/chit NCs

To prepare the NiS/chit and CdS/chit NCs, 1:1 weight ratio of MS with chitosan was selected. The chitosan was dissolved in distilled water and acetic acid. Then MS was dispersed in distilled water and added into above solution. After 24h stirring, the mixture was washed with distilled water and ethanol several times. In the final, the obtained nanocomposite was dried under vacuum at 60 ˚C for 4h. Table 1 shows different conditions for synthesizing MS nanostructures and MS/chitosan nanocomposites.

Application

The application of the nanostructures and nanocomposites was assessed by degradation of MB dye solution. In this study, 50 ml MB solution of concentration 10^{-4} ML^{-1} was added in a beaker

Table 2. Investigation of the applications of Ni and Cd sulfide/chitosan nanocomposites in the other research.

Composite	Application	Reference
$NiS@Ni_3S_2/CdS$	Photocatalyst	[21]
chitosan-Ag/NiS	anti-microbial application	[22]
CdS/chitosan	–	[23]
CdS/chitosan	Elimination of heavy metals	[24]
CdS/graphene oxide-chitosan	as an active layer for metal ion detection	[25]
CdS/chitosan	for latent fingermark detection	[26]
Silver sulfide/nickel titanate/chitosan	Photocatalyst	[27]
Nickel sulfide/chitosan	for removing toxic mercury ions	[28]

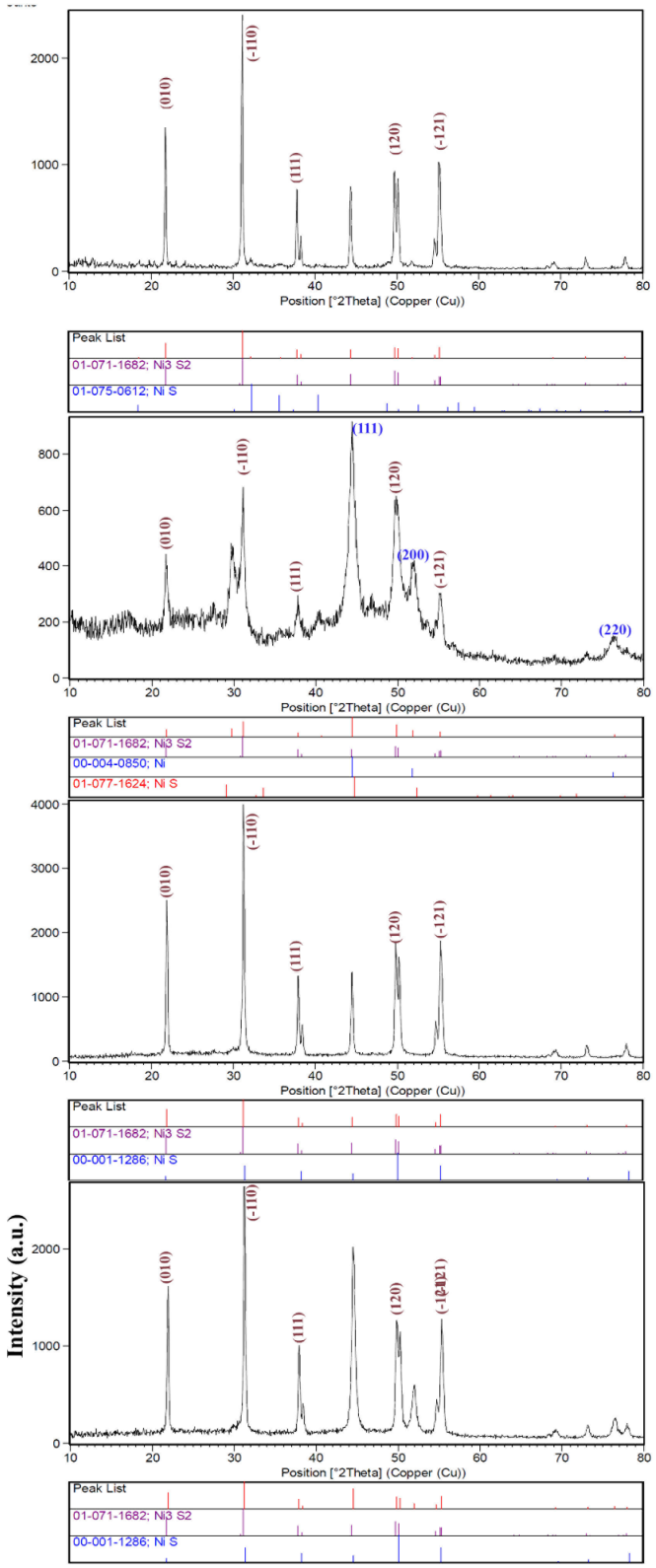

Fig. 1. XRD patterns of nickel sulfide nanostructures prepared (a) without surfactant , (b, c, d) in the presence of CTAB, PVA and PEG, respectively.

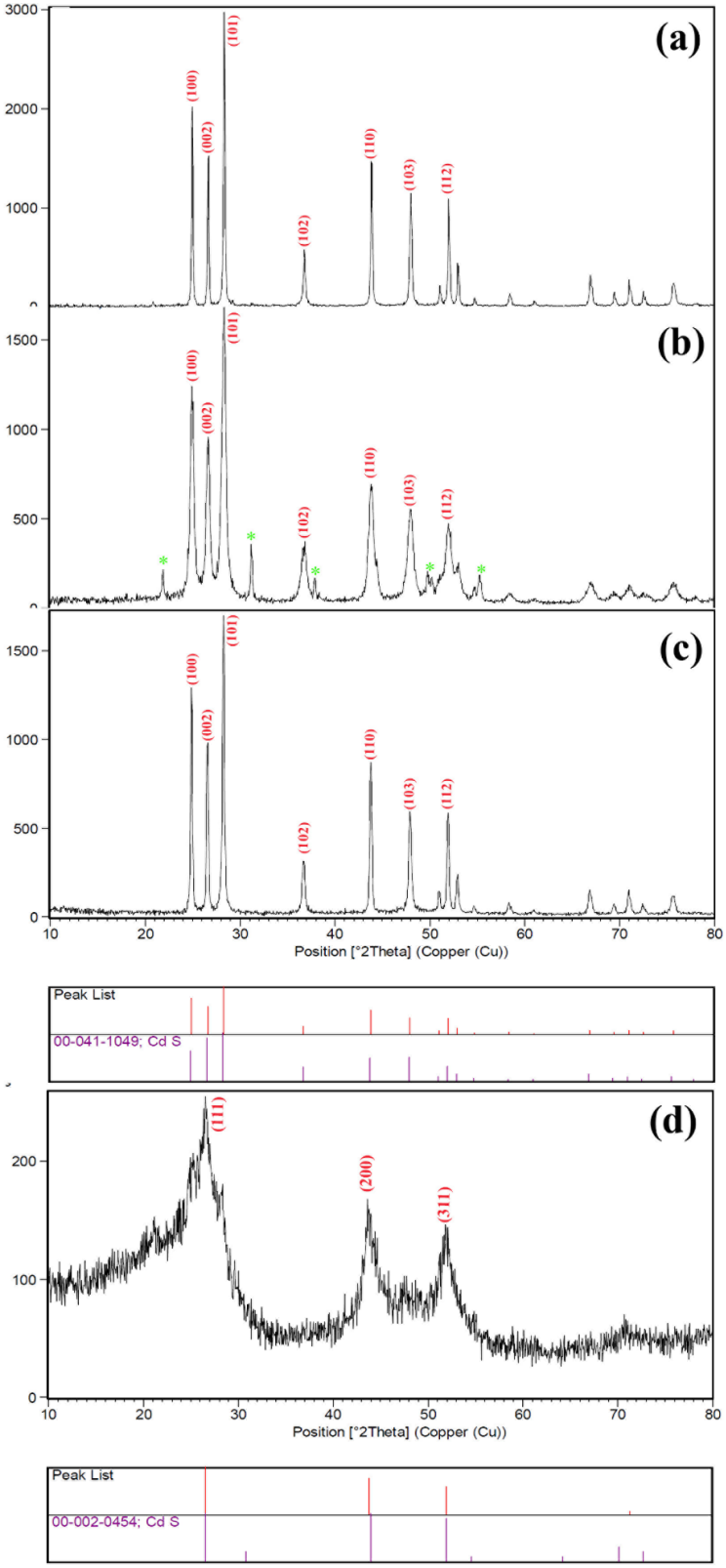

Fig. 2. XRD patterns of CdS nanostructures prepared (a) without surfactant , (b, c, d) in the presence of CTAB, PVA and PEG, respectively.

containing 10 mg of the sample and then stirred magnetically using motorized magnetic stirrer at room temperature for 30 min to attain an UV-Vis spectrum. Also, UV-Vis spectrum of the pure MB solution was taken. Table 2 shows other research about the synthesis and investigation of the applications of Ni and Cd sulfide/chitosan nanocomposites.

RESULTS AND DISCUSSION

XRD is a useful technique for characterization of purity and crystallite structures of materials. To study the structural properties, XRD patterns of the products were taken. Fig. 1 shows XRD patterns of nickel sulfide nanostructures prepared without surfactant (sample 1) and also in the presence of CTAB (sample 2), PVA (sample 3) and PEG (sample 4). As shown in this figure, the products obtained are a mixture of Ni_3S_2 and NiS. By comparing XRD patterns, it can be found that the crystallinity of the product prepared in the presence of CTAB is low, as shown in Fig. 1b, also some peaks related

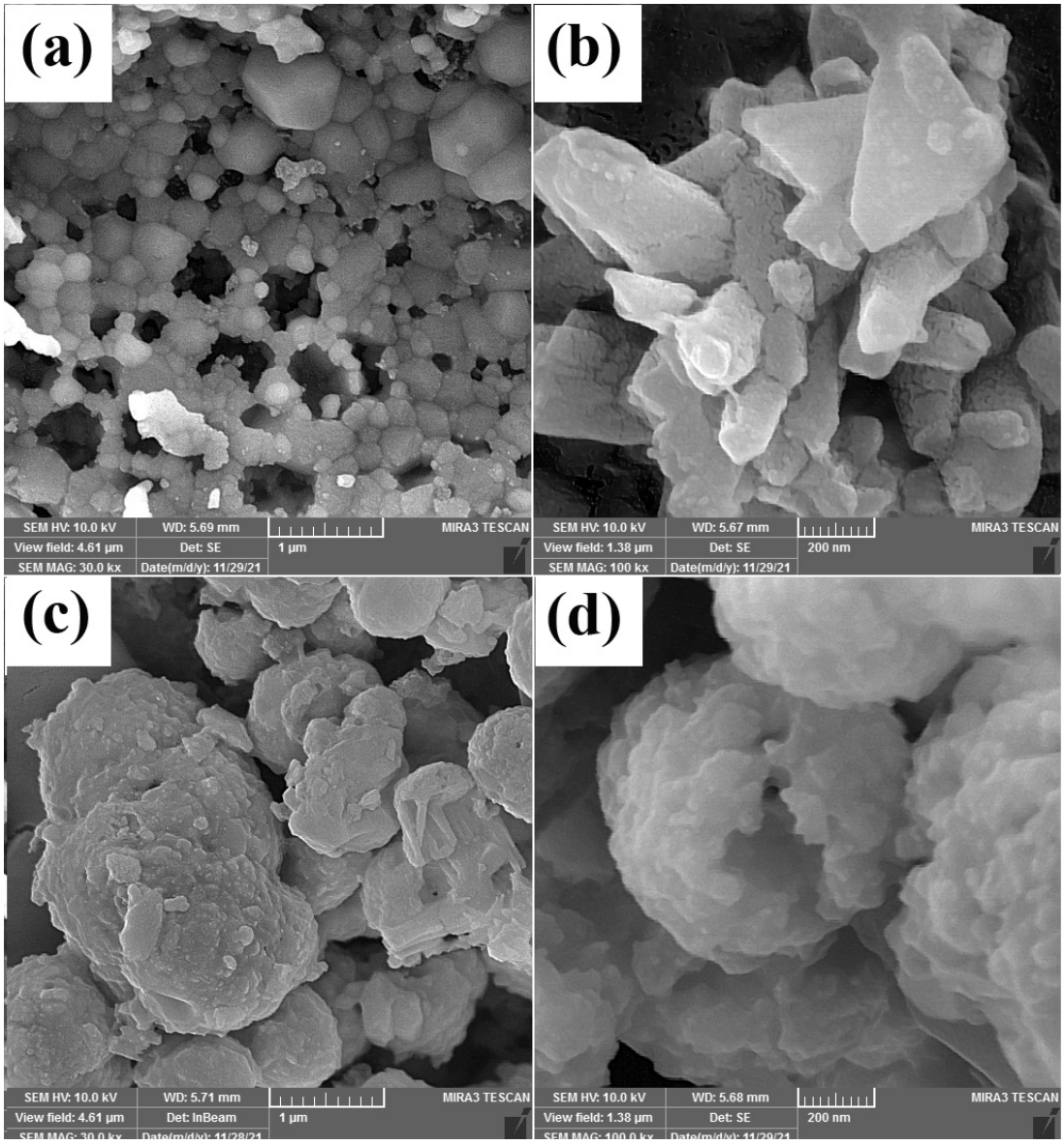

Fig. 3. SEM images of the products prepared in the absence of surfactant: (a, b) nickel sulfide (sample 1) , cadmium sulfide (sample 5).

to Ni are seen in this figure. The peaks of samples 1, 3 and 4 are sharp and long, it indicates that crystallinity of these products is high. Especially the higher intensity of the XRD peaks of sample 3 shows that the product prepared in the presence of PVA has the highest crystallinity among the samples in Fig. 1.

Fig. 2 shows XRD patterns of CdS nanostructures prepared without surfactant (sample 5) and in the presence of different surfactants. According to the patterns illustrated in this figure, the pure CdS is formed in sample 5 and also in the presence of PVA (sample 7) and PEG (sample 8). In the XRD pattern of sample 6 prepared in the presence of CTAB, in addition to CdS peaks, additional peaks related to impurity are also seen, shown with green stars in Fig. 2b. XRD patterns of samples 5, 6 and 7 are matched to the diffraction peaks of hexagonal CdS of JCPDS card number 00-041-1049. These samples were found to form well-crystallized phase based on the intensity and sharpness of its detected peaks. Using PEG as surfactant was led to the preparation of CdS with JCPDS 00-002-0454 (Fig. 2d).

The SEM images was taken to investigate the morphology of the synthesized materials. Fig. 3 shows SEM images of nickel sulfide (sample 1) and cadmium sulfide (sample 5) prepared in the absence of surfactant. Fig. 3a and b shows the formation of the polyhedral structures with a size of 50 nm to 1µm. Moreover, the agglomeration of nickel sulfide nanostructures can also be demonstrated in the SEM images. Fig. 3c and d shows formation of the agglomerated CdS spheres with diameters ranging from 500 nm to 2 µm.

To further study the morphology in samples 1 and 5, TEM and HRTEM images were taken and shown in Fig. 4. TEM image of nickel sulfide (sample 1) in Fig. 4a shows the formation of the polyhedral structures with different sizes. In HRTEM image of sample 1, various components of this sample at different magnifications are detectable, based on distance between atomic layers. This image in Fig. 4b reveals interplanar lattice spacing in sample 1 is ~ 0.5 nm. The selected area electron diffraction (SAED) pattern of this sample is shown in Fig. 4c. Also, TEM images in two different scales, including 500 nm and 100 nm of cadmium sulfide (sample

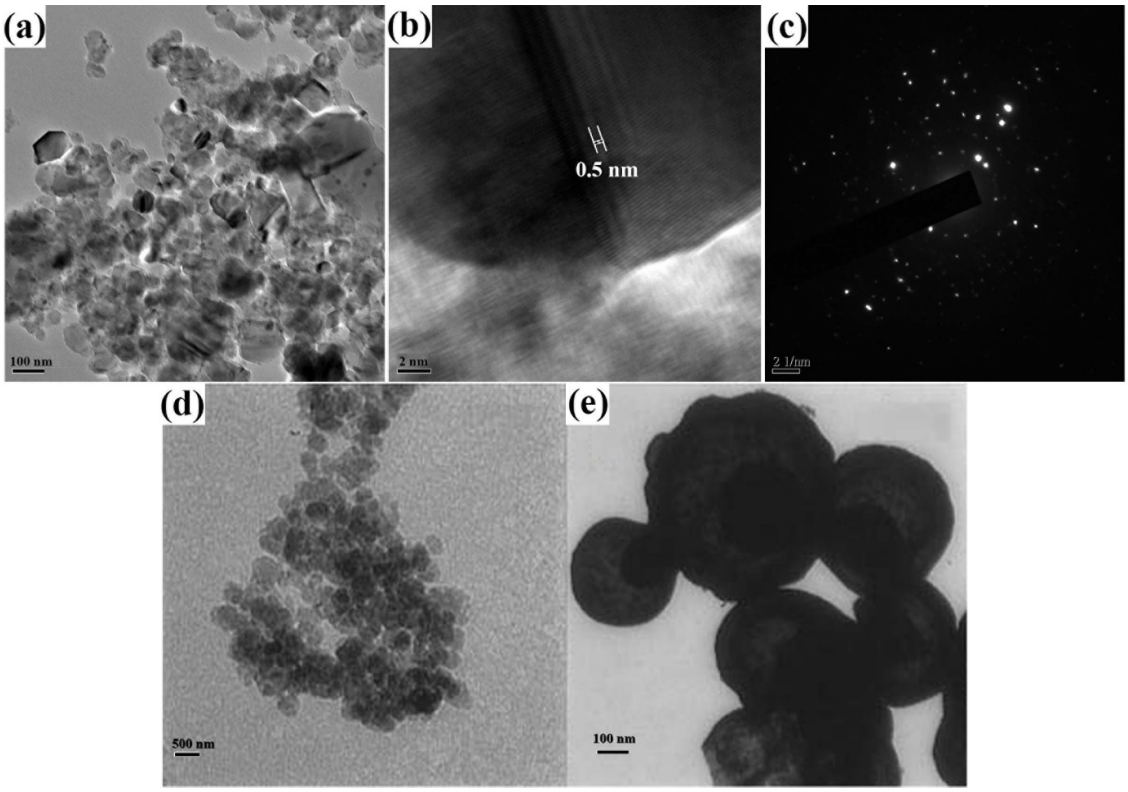

Fig. 4. (a) TEM image (b) HRTEM image and (c) SAED pattern of sample 1 , (d, f) TEM images of sample 5.

5) confirm the formation of the agglomerated CdS spheres with different diameters and confirm SEM results, (Fig. 4d and e).

IR is concerned with the vibration of molecules. There are different functional groups in molecules. The functional groups have their discrete vibrational modes in the IR spectrum. This spectrum serves as a characteristic "molecular fingerprint" and can be used to identify inorganic and organic molecules. Fig. 5 shows FT-IR spectra of cadmium and nickel sulfides. The broad absorption band nearby 3391 cm^{-1} in Fig. 5a is appointed to the stretching vibrations of absorption water. In this figure, absorption peaks at 600 and 667 cm^{-1} are because of Cd–S stretching vibration mode. The peak at 1115 cm^{-1} belong to the C–N stretching vibrations of the precursor complex and the peak at 1417 cm^{-1} belongs to O–H bending vibrations. In the case nickel sulfide (sample 1), in Fig. 5b the peaks nearby 3100–3600 cm^{-1} are assigned to the stretching vibrations of absorption water. The absorption band at 1062 cm^{-1} is appointed to the stretching vibrations of C–N band (of the precursor).

Image analysis techniques for SEM images of particles were developed to evaluate particle morphology quantitatively. Fig. 6 illustrates the surface characteristics of the nanocomposites made up of chitosan. It shows SEM images of nickel sulfide/chitosan (sample 9) and cadmium sulfide/chitosan (sample 11). The surface structure of the nanocomposites exhibits spherical morphology.

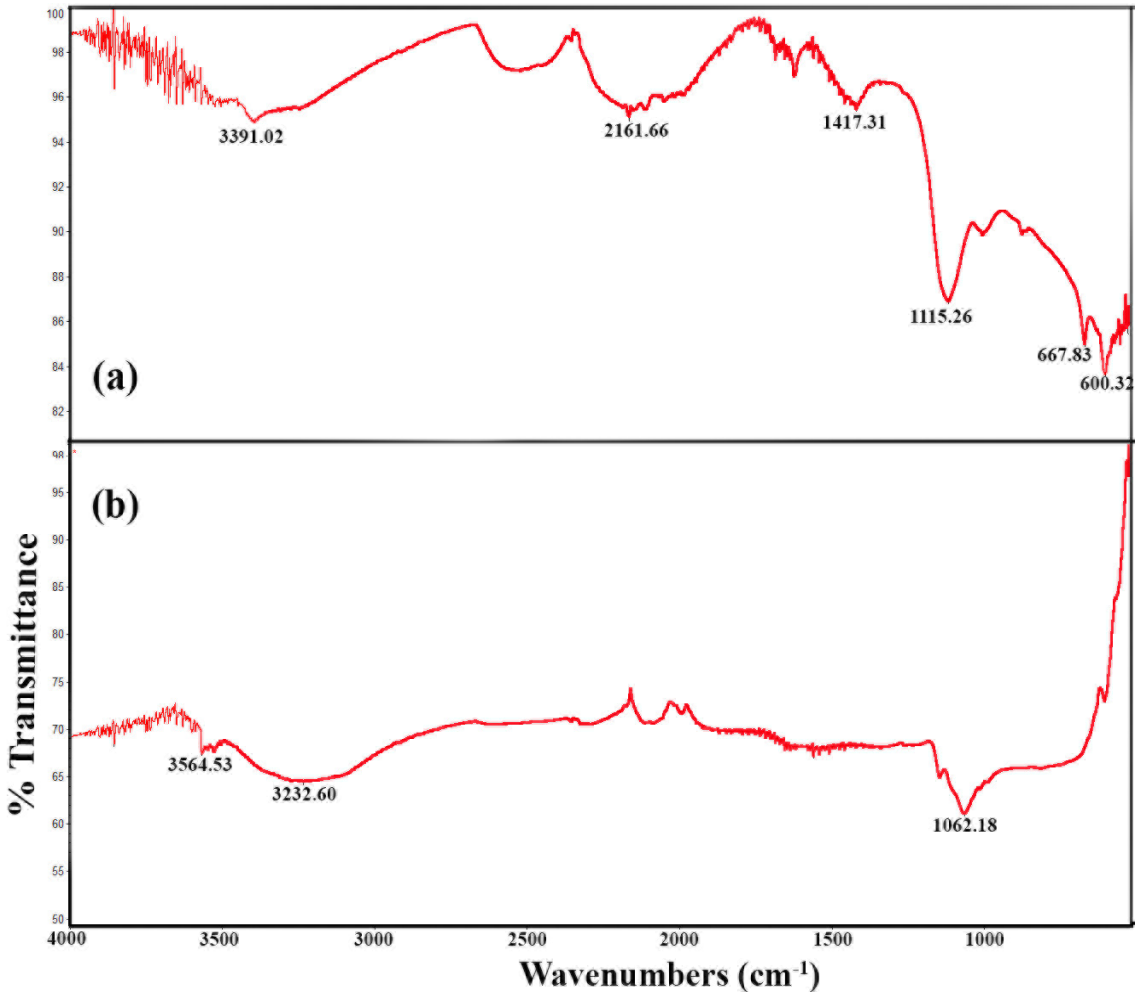

Fig. 5. FT-IR spectra of the products prepared in the absence of surfactant: (a) cadmium sulfide (sample 5) , (b) nickel sulfide (sample 1).

The spheres have been agglomerated and formed microstructures.

The EDS is one of the most versatile analytical tools for general materials analysis. Scientists use EDS to analyze and determine the elemental composition of materials. Fig. 7 depicts the EDS spectra of the nanocomposites prepared in the presence of PEG and CTAB. This figure shows Ni and S elements for samples 9 and 10, and Cd and S elements for sample 11.

UV-Vis is a spectroscopic technique that measures radiation absorption as a function of wavelength. The samples can absorb photons from a radiating field. The curve of absorption intensity

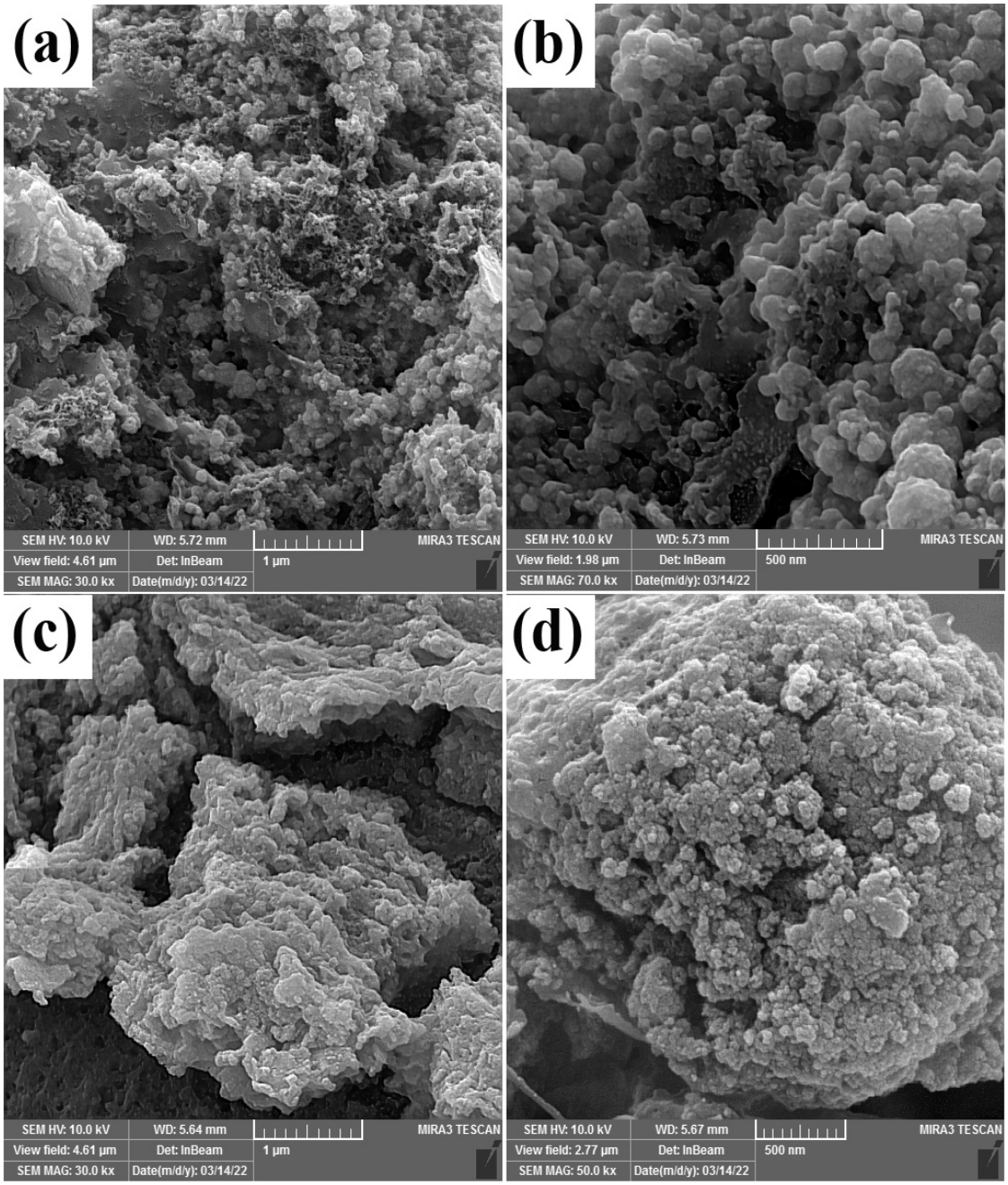

Fig. 6. SEM images of the nanocomposites prepared in the presence of CTAB: (a, b) nickel sulfide/chitosan (sample 9) , (c, d) cadmium sulfide/chitosan (sample 11).

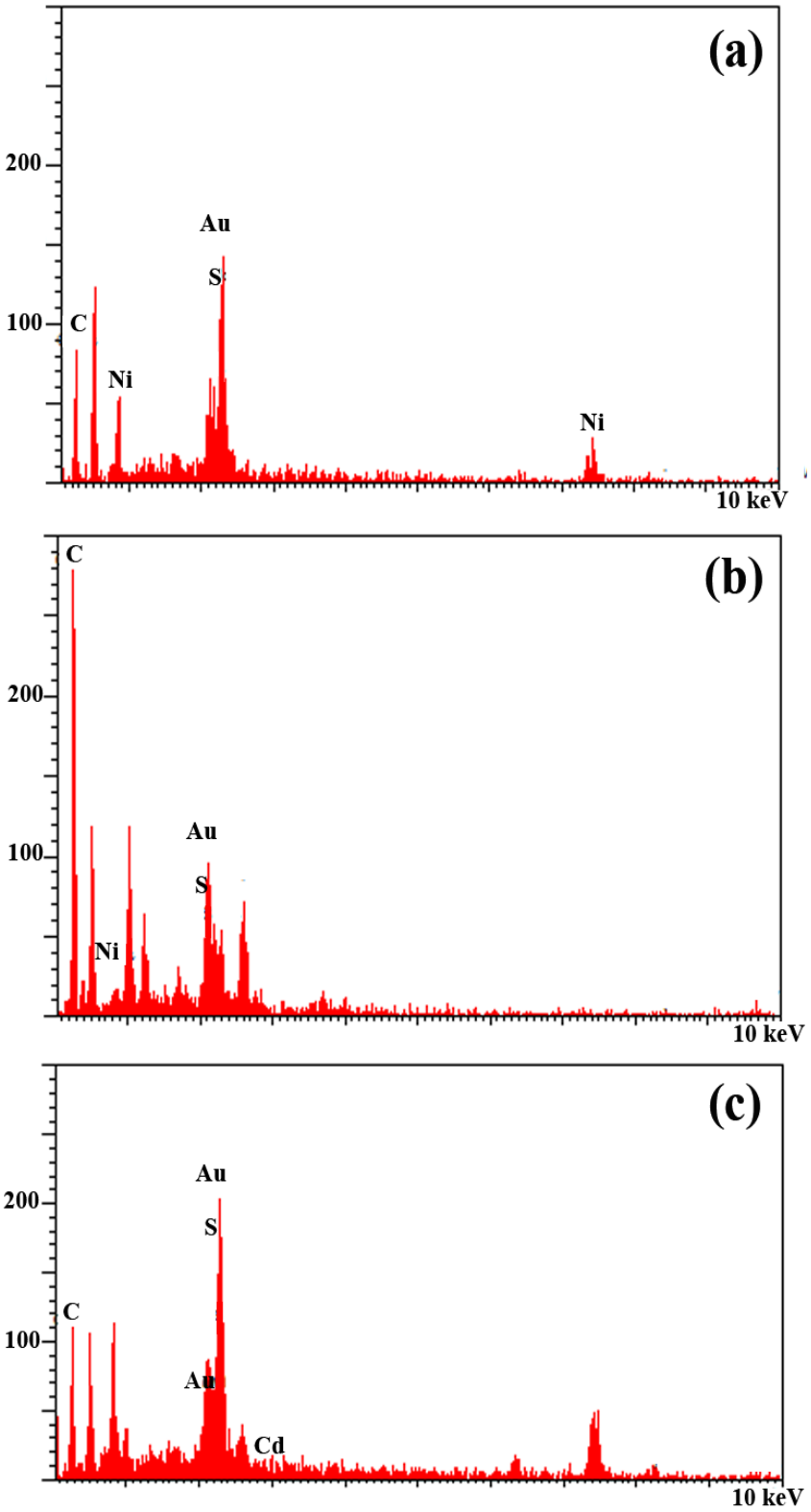

Fig. 7. EDS patterns of the nanocomposites prepared in the presence of: (a) PEG, nickel sulfide/chitosan (sample 10) , (b) CTAB, nickel sulfide/chitosan (sample 9) , (c) CTAB, cadmium sulfide/chitosan (sample 11).

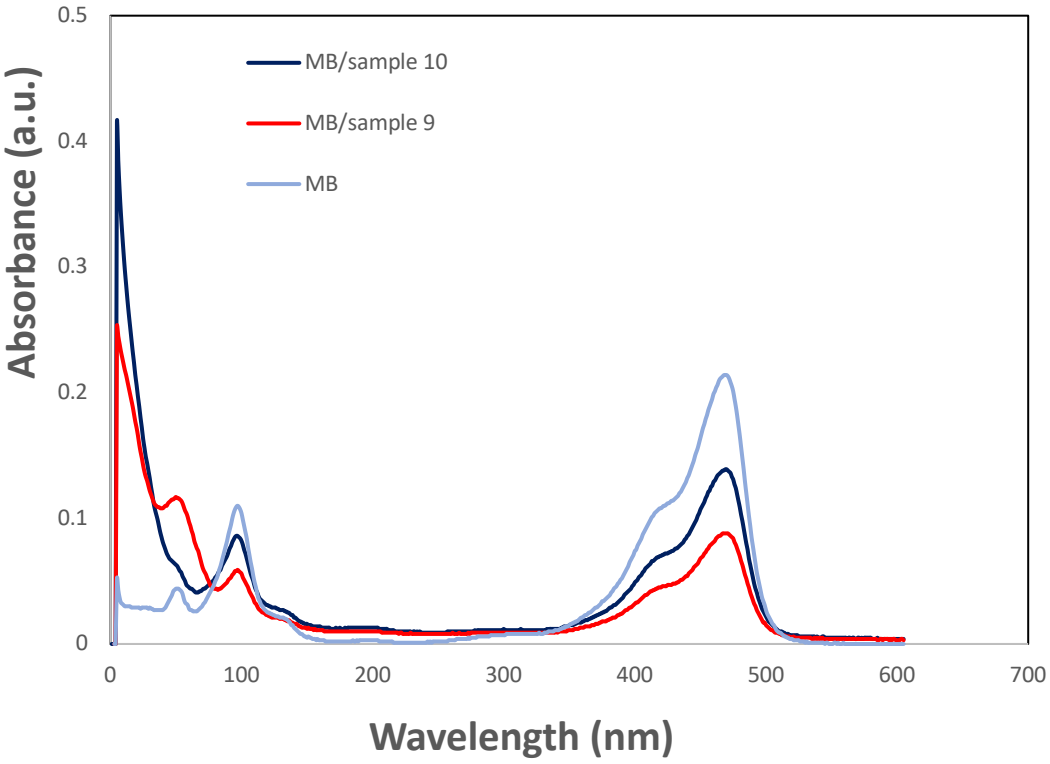

Fig. 8. Absorption spectra of MB and the solutions obtained from centrifugation of MB/samples 9 and 10 suspensions.

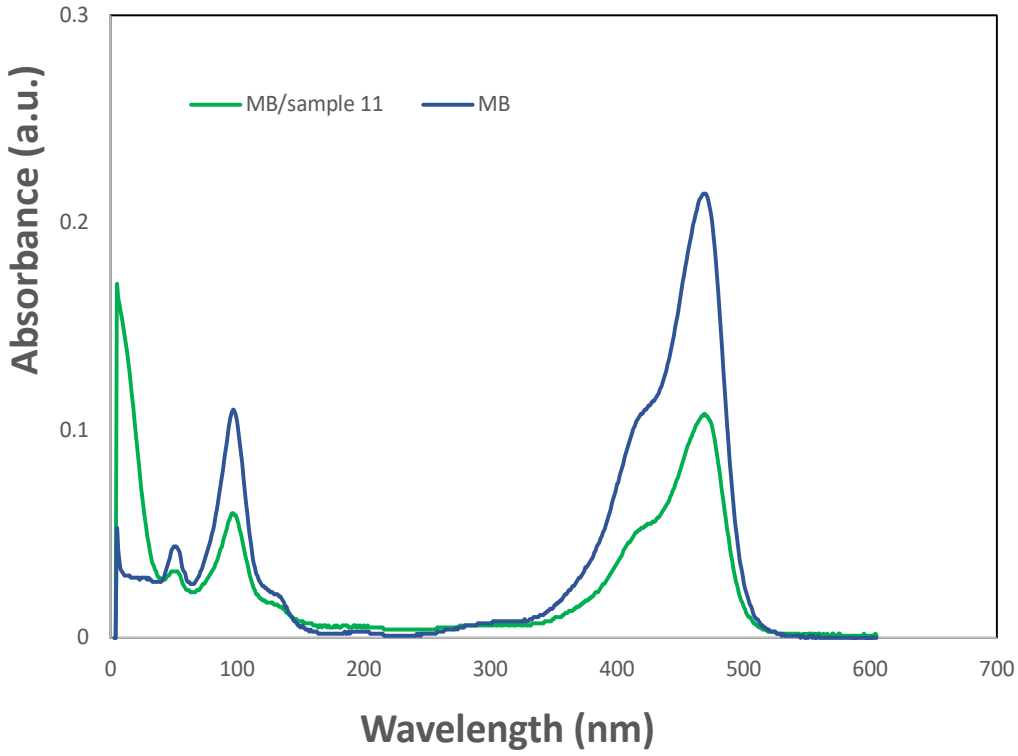

Fig. 9. Absorption spectra of MB and the solution obtained from centrifugation of MB/sample 11 suspension.

reported versus wavelength (or frequency) is named the absorption spectrum. The UV-Vis absorbance spectra of the pure MB and MB adsorbed on the surface of the nanocomposites have been shown in Fig. 8 and 9. As can see in blue curves in both figures, the absorption spectra of the MB is characterised by three main bands, one in the visible region (~470 nm), and two in ~ 100 nm and 50 nm. The results confirm the application of as-prepared nanocomposites as an effective adsorbent for MB removal from aqueous solution. The UV-Vis spectra in Fig. 8 show that the intensity of peaks of MB have been decreased after their adsorption on the surface of the nanocomposites (samples 9 and 10). The results obtained for sample 11 are similar to samples 9 and 10, as shown in Fig. 9.

CONCLUSION

In summary, MS/chit NCs were synthesized via a facile process. This process exists three steps: synthesis of the complex, synthesis of MS and synthesis of MS/chit NC. The as-prepared nanocomposites were used for MB degradation. The degradation of MB was observed in the presence of the nanocomposites under visible irradiation.

ACKNOWLEDGEMENTS

The study was supported by Kosar University of Bojnord with the grant number (NO. 0110211612).

CONFLICT OF INTEREST

The authors declare that there is no conflict of interests regarding the publication of this manuscript.

REFERENCES

1. Oviedo-Roa R, Martinez-Magadan JM, Illas F. Correlation Between Electronic Properties and Hydrodesulfurization Activity of 4d-Transition-Metal Sulfides. ChemInform. 2006;37(30).
2. Friemelt K, Lux-Steiner MC, Bucher E. Optical properties of the layered transition-metal-dichalcogenide ReS2: Anisotropy in the van der Waals plane. J Appl Phys. 1993;74(8):5266-5268.
3. Contents Volume 130 (2004). Rev Palaeobot Palynol. 2004;130(1-4):299.
4. Srivastava SK, Avasthi BN. Preparation, structure and properties of transition metal trichalcogenides. Journal of Materials Science. 1992;27(14):3693-3705.
5. Emadi H, Salavati-Niasari M, Sobhani A. Synthesis of some transition metal (M: 25Mn, 27Co, 28Ni, 29Cu, 30Zn, 47Ag, 48Cd) sulfide nanostructures by hydrothermal method. Advances in Colloid and Interface Science. 2017;246:52-74.
6. Sobhani A, Salavati-Niasari M, Hosseinpour-Mashkani SM. Single-Source Molecular Precursor for Synthesis of Copper Sulfide Nanostructures. J Cluster Sci. 2012;23(4):1143-1151.
7. Sobhani A, Salavati-Niasari M, Sobhani M. Synthesis, characterization and optical properties of mercury sulfides and zinc sulfides using single-source precursor. Mater Sci Semicond Process. 2013;16(2):410-417.
8. Wang J, Chew SY, Wexler D, Wang GX, Ng SH, Zhong S, Liu HK. Nanostructured nickel sulfide synthesized via a polyol route as a cathode material for the rechargeable lithium battery. Electrochem Commun. 2007;9(8):1877-1880.
9. Kapinus EI, Viktorova TI, Khalyavka TA. Photocatalytic activity of nanoparticles of metal sulfides in the degradation of organic dyes. Theor Exp Chem. 2006;42(5):282-286.
10. Li J, Ni Y, Liu J, Hong J. Preparation, conversion, and comparison of the photocatalytic property of Cd(OH)2, CdO, CdS and CdSe. Journal of Physics and Chemistry of Solids. 2009;70(9):1285-1289.
11. Salavati-Niasari M, Sobhani A. Single-Source Molecular Precursor for Synthesis of CdS Nanoparticles and Nanoflowers. High Temp Mater Processes (London). 2012;31(2).
12. Cui X, Li W, Ryabchuk P, Junge K, Beller M. Bridging homogeneous and heterogeneous catalysis by heterogeneous single-metal-site catalysts. Nature Catalysis. 2018;1(6):385-397.
13. Orooji Y, Nezafat Z, Nasrollahzadeh M, Kamali TA. Polysaccharide-based (nano)materials for Cr(VI) removal. Int J Biol Macromol. 2021;188:950-973.
14. Wollner A, Lange F, Schmelz H, Knozinger H. Characterization of mixed copper-manganese oxides supported on titania catalysts for selective oxidation of ammonia. Applied Catalysis A: General. 1993;94(2):181-203.
15. Amini, R., Nabiyouni, G., Jarollahi, S. Removal of azo dyes pollutants: Photo catalyst and magnetic investigation of iron oxide-zinc sulfide nanocomposites. Journal of Nanostructures, 2021; 11(1): 95-104.
16. Mousavi-Kamazani M, Rahmatolahzadeh R, Beshkar F. Facile Solvothermal Synthesis of CeO2–CuO Nanocomposite Photocatalyst Using Novel Precursors with Enhanced Photocatalytic Performance in Dye Degradation. Journal of Inorganic and Organometallic Polymers and Materials. 2017;27(5):1342-1350.
17. Zinatloo-Ajabshir S, Salavati-Niasari M, Sobhani A, Zinatloo-Ajabshir Z. Rare earth zirconate nanostructures: Recent development on preparation and photocatalytic applications. J Alloys Compd. 2018;767:1164-1185.
18. Zinatloo-Ajabshir S, Morassaei MS, Amiri O, Salavati-Niasari M. Green synthesis of dysprosium stannate nanoparticles using Ficus carica extract as photocatalyst for the degradation of organic pollutants under visible irradiation. Ceram Int. 2020;46(5):6095-6107.
19. Mousavi-Kamazani M. Facile hydrothermal synthesis of egg-like BiVO4 nanostructures for photocatalytic desulfurization of thiophene under visible light irradiation. Journal of Materials Science: Materials in Electronics. 2019;30(19):17735-17740.
20. Zhang R, Zheng D, Chen J, Zhang C, Wang C. Design of NiS@Ni3S2/CdS heterostructure with intimate contact interface for sensitive photoelectrochemical detection of lincomycin. Food Chem. 2023;418:136028.
21. Kumar BH, Okla MK, Abdel-maksoud MA, Al-Qahtani WH,

AbdElgawad H, Altukhayfi MS, et al. Chitosan capped Ag/NiS nanocomposites: A novel colorimetric probe for detection of L-cysteine at nanomolar level and its anti-microbial activity. Int J Biol Macromol. 2021;193:2054-2061.
22. Li Z, Du Y, Zhang Z, Pang D. Preparation and characterization of CdS quantum dots chitosan biocomposite. React Funct Polym. 2003;55(1):35-43.
23. K. Algethami F, Saidi I, Ben Jannet H, Khairy M, Abdulkhair BY, Al-Ghamdi YO, Abdelhamid HN. Chitosan-CdS Quantum Dots Biohybrid for Highly Selective Interaction with Copper(II) Ions. ACS Omega. 2022;7(24):21014-21024.
24. Saleviter S, Fen YW, Omar NAS, Daniyal WMEMM, Abdullah J, Zaid MHM. Structural and Optical Studies of Cadmium Sulfide Quantum Dot-Graphene Oxide-Chitosan Nanocomposite Thin Film as a Novel SPR Spectroscopy Active Layer. Journal of Nanomaterials. 2018;2018:1-8.
25. Dilag J, Kobus H, Ellis AV. Cadmium sulfide quantum dot/chitosan nanocomposites for latent fingermark detection. Forensic Sci Int. 2009;187(1-3):97-102.
26. Wang J, Sun J, Huang J, Fakhri A, Gupta VK. Synthesis and its characterization of silver sulfide/nickel titanate/chitosan nanocomposites for photocatalysis and water splitting under visible light, and antibacterial studies. Materials Chemistry and Physics. 2021;272:124990.
27. Han Y, Tao J, Khan A, Khan A, Ali N, Malik S, et al. Development of reusable chitosan-supported nickel sulfide microspheres for environmentally friendlier and efficient bio-sorptive decontamination of mercury toxicant. Environmental Science and Pollution Research. 2023;30(16):47077-47089.